Interoceptive signals shape the earliest markers and neural pathway to awareness at the visual threshold

Viviana Leupin, Juliane Britz*

Department of Psychology, University of Fribourg, P.-A. Faucigny 2, CH-1700 Fribourg, Switzerland.

* Juliane Britz

Email: juliane.britz@unifr.ch

Author Contributions: V.L. and J.B. designed research, V.L. performed research, V.L. analyzed data, V.L. and J.B. wrote manuscript

Competing Interest Statement: The authors declare no conflict of interest.

Classification: Biological Sciences, Neuroscience

Keywords (3 - 5): consciousness, brain-body interaction, EEG, cardiac phase, respiratory phase

This PDF file includes:

Main Text

Figures 1 to 4

SI Figures

Abstract

Conscious awareness for threshold-stimuli fluctuates stochastically with the pre-stimulus brain state and variations of interoceptive signals across the cardiac and respiratory cycle. It remains debated whether interoceptive signals are suppressed or not and at what stages of processing they affect awareness in different sensory modalities. Because cardiac and respiratory activity are coupled through respiratory sinus arrythmia (RSA), we investigated the influence of the cardiac (systole/diastole) and the respiratory (inhalation/exhalation) phase on awareness-related ERPs. Subjects discriminated visual threshold stimuli while their EEG, ECG and respiration were simultaneously recorded. We compared ERPs and their intracranial generators for stimuli identified correctly with and without awareness as a function of the cardiac and respiratory phase. Cyclic variations of interoceptive signals from the baroreceptors (BRs) modulated both the earliest electrophysiological markers and the trajectory of brain activity when subjects became aware of the stimuli: the P1 was the earliest marker of awareness for low (diastole/inhalation) and the VAN for high (systole/exhalation) BR activity, indicating that interoceptive signals interfere with sensory processing of the visual input. Likewise, activity spread from the anterior insula to prefrontal cortex during low and from the posterior insula to posterior parietal cortex during high BR activity, providing a new solution to the debate whether activity in prefrontal or posterior parietal cortex is crucial for awareness: these regions were differentially recruited as a function of cyclic variations of BR activity rather than task demands. Our results suggest that the cardiac and respiratory rhythms are important rhythms that shape awareness-related brain activity.

Significance Statement

The brain continuously processes stimuli from inside and outside the body, and interoceptive stimuli can modulate the perception of external stimuli. Cardiac and respiratory rhythms are important pacemakers of the organism and we show how they shape awareness-related brain activity for visual threshold stimuli in two ways. Variations of baroreceptor (BR) activity across the cardiac and respiratory cycle affect 1) the earliest electrophysiological marker (P1 for low (diastole/inhalation), VAN for high (systole/exhalation) BR activity) and 2) the brain areas

activated (frontal cortex for low and parietal cortex for high BR activity) when subjects become aware of a stimulus. We propose to consider cardiac and respiratory activity as important modulators of brain activity rather than dismissing them as noise.

Introduction

Trial-by-trial variations in brain activity modulate the response of the brain to external stimulation (1, 2) and can predict fluctuations in conscious awareness (3–5). Awareness of a stimulus requires the dynamic interplay of activity in sensory, parietal and frontal cortex (6–8), but it remains debated whether activity in a posterior occipito-temporo-parietal hot zone (9) or interactions between parietal and frontal cortex (6, 10) are crucial for awareness. Awareness also consistently recruits the insula (11), a multi-modal hub with a caudo-rostral trajectory of connections to parietal and frontal areas (12–14). The posterior insula (pI) is considered the primary visceral cortex (15) and processes interoceptive stimuli (16, 17); the anterior insula (aI) integrates sensory stimuli both from outside and inside the body (14, 18) and together with the anterior cingulate cortex (ACC) forms the main hub of the saliency network (19, 20).

The involvement of the insula in awareness and the intricate connection between brain and body can explain why conscious awareness also varies with cyclic fluctuations in bodily signals. The cardiac rhythm is an important pacemaker of the organism, and increased blood pressure in the systole activates the BRs that project to somatosensory cortex and the pI (21, 22). This ascending cascade of visceral afferents modulates the processing of external stimuli: simple visual (23–25), auditory (26) and somatosensory (27–29) stimuli are detected more readily in the diastole when the BRs are silent, and stimuli presented during the diastole elicit higher ERP amplitudes (27, 30). Another rhythmic driver of the organism is respiration whose primary physiological function is gas exchange (O_2 for CO_2), and stimulus processing also varies across the respiratory phase: emotional (31), simple somatosensory (28) and visual (32) stimuli are preferentially processed during inhalation, and subjects synchronize breathing with task demands (28, 32). Respiration can affect awareness in a direct and an indirect way: rhythmic mechanical stimulation of the olfactory bulb during inhalation directly drives the entrainment of rhythmic brain activity, and respiratory phase so modulates both oscillatory (31, 33, 34) and broad-band resting-state (35) activity. The

indirect influence of the respiratory phase on awareness is driven by RSA, i.e. the acceleration of cardiac frequency during inhalation / deceleration during exhalation. RSA is a complex phenomenon and considered as an indicator of vagal tone; it is partially modulated by the balance between the sympathetic and parasympathetic nervous system (36) and mediated by increased BR activity during exhalation to optimize oxygen uptake (37).

Despite their tight coupling, the influence of cardiac and respiratory phase on awareness-related brain activity have not been assessed jointly. We bridge this gap and investigate at what stages of processing the effects of cardiac and respiratory phase exert their influence on awareness in the visual modality. While it is clear that interoceptive stimuli from the body can modulate the processing of sensory stimuli, it remains debated how the brain separates the processing of interoceptive and sensory stimuli, i.e. whether 1) interoceptive stimuli are suppressed **(27)** or not **(38)** when subjects become aware of a sensory stimulus and 2) at what stages of processing the effects of the cardiac and respiratory phase affect awareness.

Here we investigate the effects of cardiac and respiratory phase on ERPs elicited by visual threshold stimuli when they are correctly identified with and without awareness **(3, 39)** (Fig1). We used ERPs and EEG source imaging **(40, 41)** to 1) map the time course of ERP amplitudes and their intracranial source differences to elucidate the interplay between sensory and higher cortical areas when subjects become aware of a visual stimulus and 2) to investigate the role of the cardiac and respiratory phase in this process. We discuss our findings in terms of how tonic and phasic cyclic variations in BR activity can modulate awareness-related brain activity.

=== insert Fig 1 about here ===

Results

Behavioral results

Subjects responded correctly in 85.5% (SD=6.4%) of trials with a mean ratio of correct aware/unaware responses of 50.4/49.6% (SD=11.5%); only correct responses were submitted to further analyses. Subjects responded significantly faster in the aware (719±257 ms) than the unaware (893±396 ms) condition (main effect of awareness ($F(1,29)=42.4$, $p<.001$, $\eta^2_p=0.59$).

There was no main effect of cardiac or respiratory (both *Fs*<1) phase, and neither phase interacted with awareness (both *Fs*<1) (Fig S1).

Stimulus-evoked potentials

On average, 251 trials were retained in the aware (126/125 (systole/diastole), 114/137 (inhalation/exhalation)) and 244 in the unaware (120/123 (systole/diastole), 112/132 (inhalation/exhalation)) condition in each subject. Despite being presented for only 16 ms, the stimulus elicited clearly discernible canonical ERPs.

Awareness modulates ERPs

These ERPs were significantly modulated by awareness in three time-windows reflecting early sensory (P1, 90-120ms), perceptual (VAN, 250-350ms) and post perceptual (P3/LPC, 400-600ms) processes (Fig S2). We applied the False-Discovery Rare (FDR) (42) across all 150 time-points / 128 electrodes to correct for multiple comparisons. The P1 was more positive over occipital electrodes in the aware than the unaware condition; the VAN encompasses the N2 complex and was more negative in the aware than the unaware condition over occipital and lateral temporal electrodes, and the P3/LPC component was more positive in the aware than the unaware condition over centro-parietal electrodes.

Cardiac phase modulates ERPs

The cardiac phase modulated visual ERPs (Fig S3) over occipital and lateral temporal electrodes in two time-windows: ERPs were significantly more positive in the systole than the diastole in the time-window -100-200ms and more negative in the time-window 230-550ms (Fig S3A). In the systole, the cardiac pulse wave overlaps with the stimuli that are presented within this interval (-100-200ms); in the diastole, the same cardiac pulse wave appears to occur later because it is elicited during the systole of the subsequent heartbeat (300-500ms) (Fig S3C). This effect is not caused by the cardiac field artefact (CFA), (Fig S3A).

=== insert Fig 2 about here ===

Cardiac phase modulates awareness-related ERPs

The cardiac phase differentially modulated awareness-related ERPs reflecting sensory (P1) and perceptual processes (VAN). The amplitude of the P1 peak was selectively modulated by awareness: only in the diastole, it was attenuated in the unaware relative to the aware condition (cardiac phase x awareness: ($F(1,29)=6.74$, $p=0.015$, $\eta^2_p=0.19$, Fig2B). Linear contrasts revealed a significant effect of awareness in the diastole ($t(29)=3.16$, $p=0.007$, $d=0.57$), but not the systole ($t<1$) (Fig2A). Awareness and cardiac phase did not interact during the VAN time-window, but the effect size for the contrast between aware and unaware conditions was larger in the systole than the diastole in the time-window 220-350 ms (Fig2D). The earliest marker of awareness varied with the cardiac phase: P1 (silent BRs) in the diastole and VAN (active BRs) in the diastole.

Respiratory phase modulates awareness-related ERPs

Unlike the cardiac phase, the respiratory phase did not affect ERPs. Like the cardiac phase, the respiratory phase modulated awareness-related ERPs, albeit somewhat differently. The amplitude of the ascending slope of the P1 (65-95ms) was likewise selectively modulated by awareness (respiratory phase x awareness: $F_{1,29}=4.65$, $p=0.039$, $\eta^2_p=0.14$) and attenuated in the unaware condition only during inhalation ($t(29)=3.32$, $p=0.004$, $d=0.6$) but not exhalation ($t<1$) (Fig 2E/F). Like for the cardiac phase, awareness and respiratory phase did not interact during the VAN (220-350 ms), but the effect sizes for the contrast between the aware and unaware conditions were larger during inhalation than exhalation (Figure 2H). Unlike the cardiac phase that differentially affected the P1 and the VAN, the respiratory phase affected them similarly: both were more strongly pronounced during inhalation than exhalation. However, like for the cardiac phase, the earliest marker of awareness varied with the respiratory phase: P1 during low (inhalation), and the VAN during high (exhalation) BR activity.

Stimulus-evoked sources

Cardiac phase modulates source activity underlying sensory processing

We determined the sources underlying the sensor space effects by comparing the intracranial generators during the time-windows of the significant amplitude differences of P1, VAN and P3/LPC. Unlike in sensor space, there was no main effect of awareness and no interaction between awareness and cardiac phase in the source space in the time-window of the P1 (90-120

ms). However, during that time-window, the cardiac phase differentially modulated source activity: current density was higher in the diastole than the systole in the aware ($t(29)=3.45$, $p=0.003$, $d=0.63$) but not in the unaware condition ($t(29)=1.16$, $p>.05$) (Fig3B) in a spatio-temporal cluster encompassing right extrastriate visual and enthorinal cortex (MNI(max): x=34.3, y=-73.5, z=-12, $p=.0272$, Fig3A).

=== insert Fig 3 about here ===

Cardiac and respiratory phase modulate awareness—related source activity underlying perceptual processes

Fig4(A-C) summarizes the results of the source space analyses in the time-window of the VAN (240-340ms), all results are corrected for multiple comparisons across time and space **(43)**.

During the entire VAN time-window, the main effect of awareness (higher current density in the aware than the unaware condition) was only marginally significant in a spatio-temporal cluster encompassing a posterior (pI, ventral section of the left temporo-parietal junction (TPJ): superior temporal sulcus (STS), angular gyrus (AG)) and an anterior (aI, inferior frontal gyrus (IFG)) section (p=0.082, (MNI(max): x=-48.2, y=-48.9, z=5.2), Figure 4A), and awareness neither interacted with cardiac nor respiratory phase. The main effect of awareness was significant only in the systole in the posterior section of the cluster (pI and its ventral projection targets in the TPJ; p=0.036, MNI(max): x=- 40.2, y=-60.1, z=- 10.6, Fig4A), also note larger effect size for the main effect of awareness in sensor space in the systole than diastole.

Because activity differences persisted for a long time (100ms) across the anterior and posterior sections of the cluster, we investigated the temporal evolution of source activity differences by sub-dividing the VAN time-window into an earlier (270-310 ms) and a later (310-350 ms) part corresponding to the rising and falling phase of the VAN. The main effect of awareness reached significance only in the later time-window in the anterior section (aI, IFG) and the ventral section of the TPJ (STS, AG), (p=.046, MNI(max): x=-37.6, y=15.5, z=9.8, Fig4C). In the earlier time-window, the main effect of awareness was only marginally significant in the posterior section (pI, STS, AG, p=0.083, MNI(max): x=-61.4, y=-48.1, z=15.5, Fig4B) , which was driven by a main effect of awareness with maximal activation in the pI only when BR is high (systole: p=0.021, MNI(max):

x=-32.4, y=-31.9, z=17.1 (Figure2B), exhalation: p=.046, MNI(max): x=-32.4, y=-31.9, z=17.1, (Fig4B)).

Cardiac and respiratory phase modulate awareness—related source activity underlying post-perceptual processes

Fig4D summarizes the results of the source space analyses in the P3/LPC time-window (400-500 ms). A main effect of awareness was obtained both in pI and aI and their respective dorsal projection targets in parietal (TPJ(SMG), IPL) and frontal cortices (IFG, SFG), along with medial areas extending posteriorly (Precuneus, Posterior (PCC) and Middle (MCC) Cingulate and Fusiform Gyrus (FFG)) and anteriorly (ACC, SFG); p=0.002, MNI(max): x=-11.5, y=-7.7, z=47.3) irrespective of cardiac or respiratory phase. Medial sources did not differ between conditions, but like during the VAN time-window, lateral sources differed along a posterior-anterior gradient that varied with cyclic variations of visceral input: during high BR activity, the pI is reactivated along with its dorsal projection targets in SMG and IPL in the systole (p< 0.001, (MNI(max): x=-4.1, y=-33.4, z=30.5)); aI and middle temporal gyrus (MTG) are additionally activated during exhalation (p=0.001, (MNI(max): x=-4.1, y=-33.4, z=30.5)). When BR activity is low, aI is activated along with its projection targets in IFG and ACC (inhalation, p= 0.002, (MNI(max): x=-4.1, y=-33.4, z=30.5); SFG is additionally activated during diastole (p= 0.007, (MNI(max): x=-30.8, y=9.3, z=53.6).

Discussion

We show that cyclic variations of interoceptive signals across the cardiac and the respiratory phase determine both the earliest electrophysiological markers of awareness and the trajectory of brain activity when subjects become aware of a visual threshold stimulus.

The P1 was the earliest ERP component modulated by awareness when BR activity was low (diastole, inhalation), and current density in extrastriate visual cortex was lower in the systole than the diastole when subjects saw the stimulus. This indicates that interoceptive signals from the BRs attenuate the sensory processing of a visual stimulus. The modulation of the P1 with cyclic fluctuations in interoceptive input helps to solve the controversy whether it reflects the earliest marker of awareness (44) or not (45): it does but only when concomitant interoceptive input is minimal.

The VAN was the earliest marker of awareness when BR was high (systole, exhalation). Its intracranial generators differed both across time and with cyclic variations in BR activity along a posterior to anterior gradient of spread of activation from the insula in a cluster comprising an anterior and a posterior section. The posterior section encompassed the pI and its projection targets in the ventral TPJ and was exclusively activated during the early (rising) phase of the VAN and only when BR activity was high (systole/exhalation). The pI is considered the primary interoceptive cortex (15) and is the main cortical projection target of the BRs (21, 22), and the TPJ receives and integrates multimodal inputs (46) and is considered a hub important for conscious awareness (47). When a visual stimulus is presented shortly after the heartbeat or during exhalation, both visceral and multimodal areas are activated jointly to effectively process and separate the visceral and visual inputs. We show statistically significant differences in activity between aware and unaware identification of a visual stimulus in temporal cortex in this early time-window when subjects report their percept. The global neuronal workspace (GNW) model postulates that conscious awareness can only arise if activity reaches frontal and parietal areas after ~300 ms, it also explicitly states that activity in occipital and inferior temporal areas before ~300 ms does not differ between aware and unaware perception (6, 48). These areas are activated as a function of awareness earlier than postulated by the GNW model but only when the visual stimulus is accompanied by a visceral input. The increased TPJ activity is not driven by the visual stimulus when it reaches awareness per se, but it arises from increased processing demands when a visual and a visceral stimulus occur simultaneously.

The anterior section of the cluster (aI, IFG) is activated along with the TPJ in the late (falling) phase of the VAN irrespective of the cardiac or respiratory phase. The aI integrates visceral inputs with sensory, emotional, social and cognitive information relayed from other cortical areas (49). The aI and IFG are important hubs of the SN (19, 20), which amplifies the salience of stimuli. Our findings suggest that 1) the VAN component reflects the critical transition at which salient inputs are selected and successively spread and maintained in a global conscious state, and 2) this process differs with cyclic variations in bodily signals, which can add to our understanding of the role of the insula for awareness (11).

The source differences of the LPC corroborate how cyclic variations in visceral input influence which brain areas are activated when subjects become aware of a visual stimulus. Overall, activity was stronger in widespread areas including the insula (aI, pI) and their respective dorsal and ventral projection targets along with medial areas when subjects became aware of the stimulus. However, cyclic variations of BR activity across the cardiac and respiratory phase recurrently and selectively reactivated the pI when BR activity was high (systole/exhalation) and the aI when BR activity was low (diastole/inhalation), and activity spread dorsally to parietal (from pI) and frontal (from aI) cortex when subjects become aware of the stimulus. This illustrates the modulatory role of primary visceral (pI) cortex for awareness: it is activated both by phasic (systole) and tonic (exhalation) BR activation, and its role in conscious awareness is not limited to processing visceral signals when they co-occur with an external stimulus. Rather, the configuration of activity in the insula during the VAN determines the configuration of activity during the LPC: awareness is supported by parietal cortex for high and by frontal cortex for low BR activity. Thus, none of these areas seem to be per se necessary for awareness but they can contribute independently to the awareness of stimulus. Our findings shed a new light on the debate about the roles of parietal and frontal cortex for awareness: previous studies using no-report paradigms suggest that activity in the posterior parietal hot zone reflects awareness (9) and that PFC reflects selective attention and response selection rather awareness per se when subjects overtly report their percept (6, 10). We provide a new solution to this debate and show that parietal and frontal areas are differentially recruited as a function of both phasic and tonic cyclic variations in BR activity across the cardiac and respiratory phases rather than by task demands. The activity in more domain-general areas in posterior medial cortex (PC/PCC) does not vary with fluctuations in bodily signals. Taken together, variations in BR activity influence which sub-region of the insular cortex is recruited and hence to which cluster of connected regions the activation spreads. High BR firing activates the pI in the early stage of the VAN which drives the signal to reverberate in posterior and highly connected parietal regions later on (similar to the posterior “hot zone”(9)). In phases of weaker BR activity stimulus processing is driven by the aI-IFG cluster in the later stage of the VAN from where it spreads to high-order frontal cortices (in line with GNW predictions).

The interaction between awareness and cardiac and respiratory phase is not reflected in the reaction times. Subjects do respond faster when they perceive than miss the stimulus, but not differentially across the cardiac and respiratory phases. This is most likely due to our experimental paradigm: we compared only correctly identified stimuli with and without awareness, i.e. we did not include any errors to avoid having erroneous hits. Other experiments that separately considered hits vs. misses and correct vs. error trials (27) found more hits in the diastole than systole and more errors in the systole than diastole.

Our findings suggest that visceral signals are processed and separated from the visual input rather than suppressed (27), at least when visceral and sensory signals do not share the same neuronal pathways. The heart is the first organ that develops and starts to beat rhythmically at four weeks of gestation (50). The cardiac rhythm can be considered as the first pacemaker of a mammalian organism and is fully developed by the time the neural tube starts to form (51), and we show how signals from the heart shape the neural pathway to awareness. Respiration is another fundamental bodily rhythm whose physiological function goes beyond gas exchange; it can modulate oscillatory (31, 33, 34) and broad band (35) brain activity and modulate ERPs in a visual-spatial task (32), and we show here that cyclic fluctuations of BR activity across can likewise modulate awareness-related ERPs and their sources. Subjects breathed nasally, thus respiration can affect awareness both directly through entrainment of brain activity by means of OB stimulation (31, 52) and indirectly through RSA (37). Future studies using oral respiration will be needed to differentiate between the relative contributions of these routes.

The influence of cardiac and respiratory activity on the EEG is generally dismissed as noise and eliminated (53, 54). Our demonstration of how cyclic variations of bodily signals across the cardiac and respiratory phase shape the neural pathway to awareness suggests that ECG and respiration are functionally relevant signals. They shape brain activity and affect awareness similar to trial-by-trial fluctuations in brain activity that are no longer eliminated as noise but considered to carry functional relevance. We propose to record cardiac and respiratory activity along with EEG as potentially important modulators of brain activity to open up new avenues to elucidate the intricate brain-body-connection.

Materials and Methods

Participants

Thirty-eight healthy right-handed subjects (23 female, age: 24.42 ± 4.87 years, range 18-42) participated in the EEG study. None reported a history of neurological, psychiatric, cardiological and respiratory impairments and all were right-handed **(55)**. For seven subjects no discrimination threshold could be determined, and data from one subject was rejected because of compromised data quality. The data of 30 subjects (17 female, age 25.23±5.42, range 18-42) was submitted to further analysis. Participants received monetary compensation (20 CHF/hour) or course credits after given written informed consent approved by the Ethics Committee of the University of Fribourg.

Stimuli and procedure

Stimuli were Gabor gratings subtending a visual angle of 5° (3 cpd) oriented left (135°) or right (45°) embedded in grayscale random dot noise. All stimuli were generated and presented using Psychopy3 **(56)** on a grey background on a ViewPixx Screen (1920 × 1080 pixel resolution, 120 Hz). Subjects were positioned on a chin rest 70 cm from the screen in a dimly lit room and performed the task while breathing through their nose; a piece of surgical tape was lightly placed over their mouth to prevent them from breathing orally.

First, a fixation cross was presented (700-1500 ms), followed by a blank screen for 100–300 ms and the target for 16 ms. Subjects first reported the perceived orientation by pressing the "F" (left index) or "J" (right index) key on a keyboard, (objective measure of accuracy) and then to indicate whether they saw ("J") the stimulus or not ("F") (subjective measure of awareness).

Prior to the EEG experiment, the perceptual threshold was titrated: the strength of the Gabor grating and the opacity of the random dot mask remained constant, and visibility was controlled by linearly varying the Michelson contrast of the random dot noise in 20 steps (57). Noise contrast levels that yielded an overall high accuracy (>80%) and roughly equal numbers of correct identification with and without awareness were retained for the EEG experiment. To control for threshold stability, the noise contrast could be adjusted if necessary, and 960 stimuli were presented in 12 blocks of 80 trials.

Electrophysiological Recordings Data Preprocessing

EEG was recorded from 128 active Ag/AgCl electrodes (BioSemi®) referenced to the CMS-DRL ground. The electrocardiogram (ECG) and respiration were recorded as external bipolar channels using a bipolar montage (right clavicle/lower left rib) and a breathing belt (SleepSense®) placed on the lower abdomen. All physiological signals were simultaneously recorded at 1024Hz/16 bit.

Only correct responses with (aware) and without (unaware) awareness were analyzed. Trials were classified according to the cardiac (systole/diastole) and respiratory (inhalation/exhalation) phase that were identified using the Python Neurokit2 toolbox (58). Markers were placed on the R-peak and the end of the T-wave, denoting the beginning of systole and diastole. Because the diastole can be almost twice as long as the systole, we equalized their durations to have equal numbers of trials by only retaining stimuli falling within the interval at the end of the diastole corresponding to the duration of the systole in that cycle (27). Likewise, the peaks and troughs of the respiration trace were marked to denote the periods of inhalation and exhalation. Respiratory cycles 2.5 standard deviations faster or 1.5 standard deviations slower than the mean were excluded from further analyses.

All EEG analyses (pre-processing, averaging, source modeling and statistical analyses) were performed using the MNE-python toolbox version 0.24.0.1 (59). First, the EEG signal was algebraically re-referenced to the common average reference, filtered between 0.5 and 40 Hz (FIR filter, transition window of 10 Hz) and down-sampled to 256 Hz. Oculomotor and myogenic artifacts were removed using independent component analysis (ICA) (60). Trials contaminated by ocular artifacts occurring 300 ms before and after stimulus onset were rejected, all other oculomotor and myogenic artifacts were corrected by removing the respective ICs. To investigate the potential contribution of the CFA, we separately created and analyzed a dataset retaining and excluding the CFA ICs. Next, the data was epoched between -200 ms to 1000 ms around stimulus onset, and artifact rejection and channel interpolation was performed in a data-driven way using the Autoreject procedure (61) implemented in MNE.

Analysis of behavioral data

Only correct responses with and without awareness were analyzed, and outliers (reaction times longer than the 95th and shorter than the 2nd percentile) were omitted. We used repeated measures 2 x 2 ANOVAs to separately investigate the effects of awareness (aware/unaware), cardiac (systole/diastole) and respiratory (inhalation/exhalation) phase on the reaction times and on the number of trials in each condition.

Analysis of stimulus-evoked potentials

The epoched data were averaged separately for each condition in each subject. We used mass univariate ANOVAs to assess statistical differences in ERP amplitudes as a function of the experimental factors awareness and cardiac or respiratory phase in the time-window -100-500ms around stimulus onset.

We made no a-priori assumptions for either localization or timing of effects and used FDR to correct for multiple comparisons across time and space. Subsequently, we used the time-windows and electrode locations of the significant effects obtained in the ANOVAs as regions of interest (ROIs) for which we assessed the direction of significant differences between experimental conditions using mass-univariate paired-t-tests.

Analysis of stimulus-evoked sources

We computed the intracranial generators of the stimulus-evoked responses at each time point and for each experimental condition in each subject with the dSPM inverse solution **(62)** implemented in MNE. The source space was defined in a surface-based template of the cerebral cortex (FsAverage) **(63)** comprising 5124 solution points spaced equidistantly throughout the surface of the cortical gray matter. The forward model was solved using a realistic three-layer (brain, skull, scalp) boundary-element head model to construct the lead field. The spherical electrode coordinates provided by MNE were co-registered with the scalp surface, and finally, the inverse operator was applied to the evoked responses to obtain the source time course separately for each condition in each subject.

We restricted the statistical analysis of source differences to the time-windows corresponding to significant sensor-space differences (P1, VAN, P3/LPC). In the so-defined time-windows, we

performed time-point-wise ANOVAs with the factors awareness and cardiac phase and awareness and respiratory phase, respectively. We used spatio-temporal cluster-based permutation tests to correct for multiple comparison correction across time and space (64).

Acknowledgments

This research was funded by Swiss National Science Foundation grant 10001C_189408 to J.B. We thank Roberto Caldara for providing the lab infrastructure and Alen Jelusic, Dunja Vulliemin, Amira El Hachimi, Jade Ueberschaer, Samuel Müller, Fania Maffeis and David Elmiger for help with data collection.

References

1. A. Arieli, A. Sterkin, A. Grinvald, A. Aertsen, Dynamics of Ongoing Activity: Explanation of the Large Variability in Evoked Cortical Responses. *Science* **273**, 1868–1871 (1996).

2. M. Tsodyks, T. Kenet, A. Grinvald, A. Arieli, Linking Spontaneous Activity of Single Cortical Neurons and the Underlying Functional Architecture. *Science* **286**, 1943–1946 (1999).

3. J. Britz, L. Diaz Hernandez, T. Ro, C. M. Michel, EEG-microstate depedent emergence of perceptual awareness. *Front. Behav. Neurosci.* **8**, 1–10 (2014).

4. J. Britz, C. M. Michel, State-dependent visual processing. *Front. Psychol.* **2** (2011).

5. N. A. Busch, J. Dubois, R. VanRullen, The Phase of Ongoing EEG Oscillations Predicts Visual Perception. *J. Neurosci.* **29**, 7869–7876 (2009).

6. S. Dehaene, J.-P. Changeux, L. Naccache, J. Sackur, C. Sergent, Conscious, preconscious, and subliminal processing: a testable taxonomy. *Trends Cogn. Sci.* **10**, 204–211 (2006).

7. V. A. F. Lamme, Towards a true neural stance on consciousness. *Trends Cogn. Sci.* **10**, 494–501 (2006).

8. E. D. Lumer, G. Rees, Covariation of activity in visual and prefrontal cortex associated with subjective visual perception. *Proc. Natl. Acad. Sci. USA* **96**, 1669–1673 (1999).

9. C. Koch, M. Massimini, M. Boly, G. Tononi, Neural correlates of consciousness: progress and problems. *Nat. Rev. Neurosci.* **17**, 307–321 (2016).

10. S. Dehaene, C. Sergent, J.-P. Changeux, A neuronal network model linking subjective reports and objective physiological data during conscious perception. *Proc. Natl. Acad. Sci. U. S. A.* **100**, 8520–8525 (2003).

11. P. Sterzer, A. Kleinschmidt, Anterior insula activations in perceptual paradigms: often observed but barely understood. *Brain Struct. Funct.* **214**, 611–622 (2010).

12. L. Cerliani, *et al.*, Probabilistic tractography recovers a rostrocaudal trajectory of connectivity variability in the human insular cortex. *Hum. Brain Mapp.* **33**, 2005–2034 (2012).

13. L. L. Cloutman, R. J. Binney, M. Drakesmith, G. J. M. Parker, M. A. Lambon Ralph, The variation of function across the human insula mirrors its patterns of structural connectivity: Evidence from in vivo probabilistic tractography. *NeuroImage* **59**, 3514–3521 (2012).

14. L. Q. Uddin, J. S. Nomi, B. Hebert-Seropian, J. Ghaziri, O. Boucher, Structure and function of the human insula. *J. Clin. Neurophysiol. Off. Publ. Am. Electroencephalogr. Soc.* **34**, 300–306 (2017).

15. A. D. Craig, How do you feel? Interoception: the sense of the physiological condition of the body. *Nat. Rev. Neurosci.* **3**, 655–666 (2002).

16. H. D. Critchley, C. J. Mathias, R. J. Dolan, Neuroanatomical basis for first- and second-order representations of bodily states. *Nat. Neurosci.* **4**, 207–212 (2001).

17. H. D. Critchley, S. Wiens, P. Rotshtein, A. Öhman, R. J. Dolan, Neural systems supporting interoceptive awareness. *Nat. Neurosci.* **7**, 189–195 (2004).

18. N. Gogolla, The insular cortex. *Curr. Biol.* **27**, R580–R586 (2017).

19. V. Menon, L. Q. Uddin, Saliency, switching, attention and control: a network model of insula function. *Brain Struct. Funct.* **214**, 655–667 (2010).

20. W. W. Seeley, *et al.*, Dissociable Intrinsic Connectivity Networks for Salience Processing and Executive Control. *J. Neurosci.* **27**, 2349–2356 (2007).

21. Z.-H. Zhang, S. M. Oppenheimer, Baroreceptive and somatosensory convergent thalamic neurons project to the posterior insular cortex in the rat. *Brain Res.* **861**, 241–256 (2000).

22. Z.-H. Zhang, S. M. Oppenheimer, Electrophysiological evidence for reciprocal insulo-insular connectivity of baroreceptor-related neurons. *Brain Res.* **863**, 25–41 (2000).

23. J. E. Birren, P. V. Cardon, S. L. Phillips, Reaction Time as a Function of the Cardiac Cycle in Young Adults. *Science* **140**, 195–196 (1963).

24. L. Pramme, M. F. Larra, H. Schächinger, C. Frings, Cardiac cycle time effects on mask inhibition. *Biol. Psychol.* **100**, 115–121 (2014).

25. C. Sandman, T. McCanne, D. N. Kaiser, B. Diamond, Heart rate and cardiac phase influences on visual perception. *J. Comp. Physiol. Psychol.* (1977) https:/doi.org/10.1037/H0077302.

26. A. Schulz, *et al.*, Cardiac modulation of startle: Effects on eye blink and higher cognitive processing. *Brain Cogn.* **71**, 265–271 (2009).

27. E. Al, *et al.*, Heart–brain interactions shape somatosensory perception and evoked potentials. *Proc. Natl. Acad. Sci.* **117**, 10575–10584 (2020).

28. M. Grund, *et al.*, Respiration, Heartbeat, and Conscious Tactile Perception. *J. Neurosci.* **42**, 643–656 (2022).

29. P. Motyka, *et al.*, Interactions between cardiac activity and conscious somatosensory perception. *Psychophysiology* **56**, e13424 (2019).

30. B. B. Walker, C. A. Sandman, Visual Evoked Potentials Change as Heart Rate and Carotid Pressure Change. *Psychophysiology* **19**, 520–527 (1982).

31. C. Zelano, *et al.*, Nasal Respiration Entrains Human Limbic Oscillations and Modulates Cognitive Function. *J. Neurosci.* **36**, 12448–12467 (2016).

32. O. Perl, *et al.*, Human non-olfactory cognition phase-locked with inhalation. *Nat. Hum. Behav.* **3**, 501–512 (2019).

33. J. Ito, *et al.*, Whisker barrel cortex delta oscillations and gamma power in the awake mouse are linked to respiration. *Nat. Commun.* **5**, 3572 (2014).

34. S. Varga, D. H. Heck, Rhythms of the body, rhythms of the brain: Respiration, neural oscillations, and embodied cognition. *Conscious. Cogn.* **56**, 77–90 (2017).

35. D. S. Kluger, J. Gross, Respiration modulates oscillatory neural network activity at rest. *PLOS Biol.* **19**, e3001457 (2021).

36. P. Grossman, E. W. Taylor, Toward understanding respiratory sinus arrhythmia: Relations to cardiac vagal tone, evolution and biobehavioral functions. *Biol. Psychol.* **74**, 263–285 (2007).

37. G. G. Berntson, J. T. Cacioppo, K. S. Quigley, Respiratory sinus arrhythmia: Autonomic origins, physiological mechanisms, and psychophysiological implications. *Psychophysiology* **30**, 183–196 (1993).

38. H.-D. Park, S. Correia, A. Ducorps, C. Tallon-Baudry, Spontaneous fluctuations in neural responses to heartbeats predict visual detection. *Nat. Neurosci.* **17**, 612–618 (2014).

39. R. Eklund, S. Wiens, Visual awareness negativity is an early neural correlate of awareness: A preregistered study with two Gabor sizes. *Cogn. Affect. Behav. Neurosci.* **18**, 176–188 (2018).

40. Christoph. M. Michel, T. Koenig, D. Brandeis, L. Gianotti, J. Wackermann, *Electrical Neuroimaging* (Cambridge University Press, 2009).

41. C. M. Michel, M. M. Murray, Towards the utilization of EEG as a brain imaging tool. *Neuroimage* **61**, 371–385 (2012).

42. Y. Benjamini, Y. Hochberg, Controlling the False Discovery Rate: A Practical and Powerful Approach to Multiple Testing. *J. R. Stat. Soc. Ser. B Methodol.* **57**, 289–300 (1995).

43. E. Maris, R. Oostenveld, Nonparametric statistical testing of EEG- and MEG-data. *J. Neurosci. Methods* **164**, 177–190 (2007).

44. D. Pins, D. ffytche, The Neural Correlates of Conscious Vision. *Cereb. Cortex* **13**, 461–474 (2003).

45. D. Lamy, M. Salti, Y. Bar-Haim, Neural Correlates of Subjective Awareness and Unconscious Processing: An ERP Study. *J. Cogn. Neurosci.* **21**, 1435–1446 (2009).

46. R. B. Mars, *et al.*, Connectivity-based subdivisions of the human right "temporoparietal junction area": evidence for different areas participating in different cortical networks. *Cereb. Cortex N. Y. N 1991* **22**, 1894–1903 (2012).

47. T. W. Webb, K. M. Igelström, A. Schurger, M. S. A. Graziano, Cortical networks involved in visual awareness independent of visual attention. *Proc. Natl. Acad. Sci. U. S. A.* **113**, 13923–13928 (2016).

48. S. Dehaene, J.-P. Changeux, Experimental and Theoretical Approaches to Conscious Processing. *Neuron* **70**, 200–227 (2011).

49. (Bud) Craig, A. D, How do you feel — now? The anterior insula and human awareness. *Nat. Rev. Neurosci.* **10**, 59–70 (2009).

50. H. Kidokoro, S. Yonei-Tamura, K. Tamura, G. C. Schoenwolf, Y. Saijoh, The heart tube forms and elongates through dynamic cell rearrangement coordinated with foregut extension. *Development* **145**, dev152488 (2018).

51. T. w. Sadler, Embryology of neural tube development. *Am. J. Med. Genet. C Semin. Med. Genet.* **135C**, 2–8 (2005).

52. N. Karalis, A. Sirota, Breathing coordinates cortico-hippocampal dynamics in mice during offline states. *Nat. Commun.* **13**, 467 (2022).

53. N. Gebodh, *et al.*, Inherent physiological artifacts in EEG during tDCS. *NeuroImage* **185**, 408–424 (2019).

54. S. Devuyst, T. Dutoit, P. Stenuit, M. Kerkhofs, E. Stanus, Removal of ECG artifacts from EEG using a modified independent component analysis approach in *2008 30th Annual International Conference of the IEEE Engineering in Medicine and Biology Society*, (2008), pp. 5204–5207.

55. R. C. Oldfield, The assessment and analysis of handedness: The Edinburgh inventory. *Neuropsychologia* **9**, 97–113 (1971).

56. J. Peirce, *et al.*, PsychoPy2: Experiments in behavior made easy. *Behav. Res. Methods* **51**, 195–203 (2019).

57. J. Samaha, J. J. Barrett, A. D. Sheldon, J. J. LaRocque, B. R. Postle, Dissociating Perceptual Confidence from Discrimination Accuracy Reveals No Influence of Metacognitive Awareness on Working Memory. *Front. Psychol.* **7** (2016).

58. D. Makowski, *et al.*, NeuroKit2: A Python toolbox for neurophysiological signal processing. *Behav. Res. Methods* **53**, 1689–1696 (2021).

59. A. Gramfort, *et al.*, MEG and EEG data analysis with MNE-Python. *Front. Neurosci.* **0** (2013).

60. A. Hyvärinen, E. Oja, Independent component analysis: algorithms and applications. *Neural Netw.* **13**, 411–430 (2000).

61. M. Jas, D. A. Engemann, Y. Bekhti, F. Raimondo, A. Gramfort, Autoreject: Automated artifact rejection for MEG and EEG data. *NeuroImage* **159**, 417–429 (2017).

62. A. M. Dale, *et al.*, Dynamic statistical parametric mapping: combining fMRI and MEG for high-resolution imaging of cortical activity. *Neuron* **26**, 55–67 (2000).

63. B. Fischl, M. I. Sereno, A. M. Dale, Cortical Surface-Based Analysis: II: Inflation, Flattening, and a Surface-Based Coordinate System. *NeuroImage* **9**, 195–207 (1999).

64. O. B. Kolozsvári, W. Xu, P. H. T. Leppänen, J. A. Hämäläinen, Top-Down Predictions of Familiarity and Congruency in Audio-Visual Speech Perception at Neural Level. *Front. Hum. Neurosci.* **13** (2019).

Figures

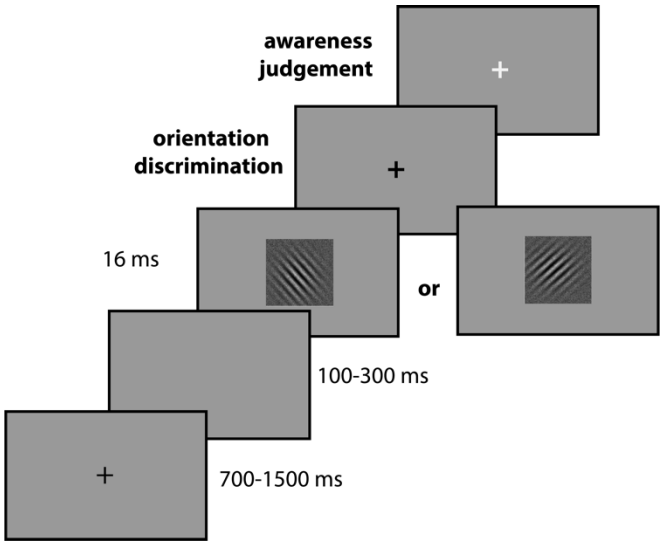

Fig 1. Experimental procedure**.** A Gabor grating either oriented to the left or to the right was presented for 16 ms. Subjects first reported the orientation of the stimulus (objective measure of accuracy) and then whether they saw the stimulus or whether they guessed (subjective measure of awareness).

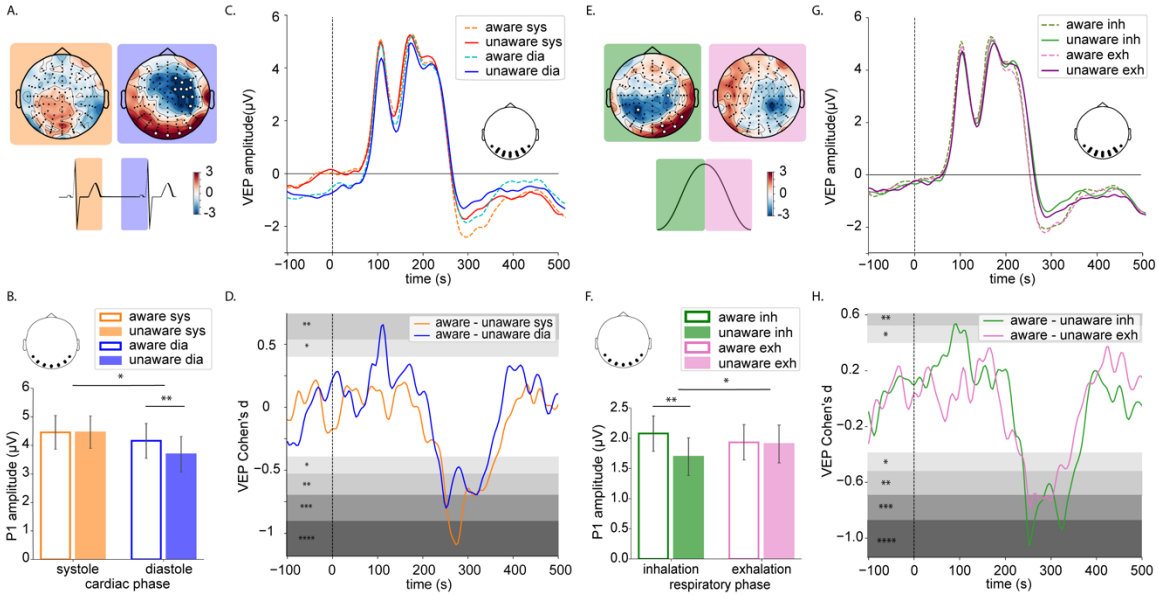

Fig 2. Modulation of the P1 and of the VAN as a function of awareness and cardiac and respiratory phase. (A) Topoplots of t-values for the contrast between aware and unaware conditions in the P1 time-window (90-120ms) in the systole (orange) and diastole (blue). Electrodes showing a significant interaction between awareness and cardiac phase are highlighted by white dots (FDR-corrected across all 150 timepoints and all 128 electrodes). (B) Significant interaction between awareness and cardiac phase on the P1 amplitude (90-120ms) averaged across occipital electrodes highlighted in the inset; error bars represent the standard error; *p<0.05, **p<0.01. (C) Grand Average ERP waveforms in all four conditions averaged across the electrodes showing a main effect of awareness in the time-window of the VAN (250-350ms) displayed in the inset. (D) Time-course of Cohen's d effect sizes for the contrast aware - unaware in the systole (orange) and diastole (blue) at the electrodes highlighted in the inset in panel (C); gray shades indicate significance levels: *p<0.05, * p<0.01, ***p<0.001, ****p< 0.0001. (E) Topoplots of t-values for the contrast between aware and unaware conditions in the P1 time-window (65-95ms) during inhalation (green) and exhalation (pink). Electrodes showing a significant interaction between awareness and respiratory phase are highlighted by white dots (FDR-corrected over the entire time-window (-100-500 ms) and all 128 electrodes). (F) Significant interaction between awareness and respiratory phase on the P1 amplitude (65-95ms) averaged across occipital electrodes highlighted in the inset; error bars represent the standard error;

*p<0.05, **p<0.01. (G) ERP waveforms in all four conditions averaged across the electrodes showing a main effect of awareness in the time-window of the VAN (250-350 ms) displayed in the inset. (H) Time-course of Cohen's d effect sizes for the contrast aware - unaware during inhalation (green) and exhalation (pink) at the electrodes highlighted in the inset in panel (G); gray shades indicate significance levels: *p<0.05, **p<0.01, ***p<0.001, ****p<0.0001

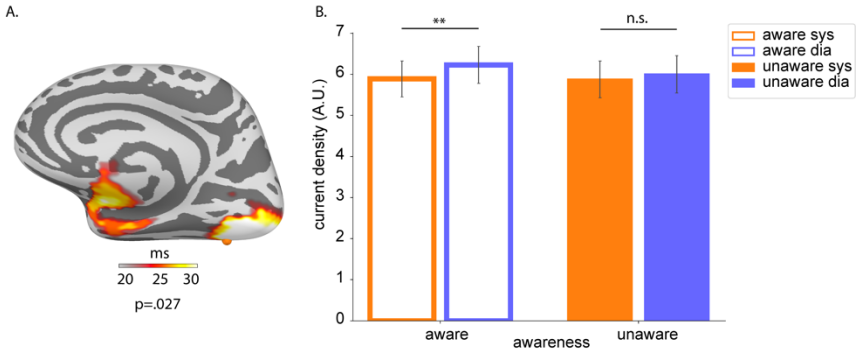

Fig 3. Current density differences in extrastriate cortex underlying the interaction between awareness and cardiac phase during the P1. (A) Statistically significant difference in current density in the aware condition between diastole and systole rendered on the FsAverage template; the color bar indicates the duration of significance (> 20ms at p=0.027) for each point in the cluster; the orange dot indicates the location of maximal activation duration (x=-34.3, y=-73.5, z=-12 mm). (B) Current density averaged across all points in the cluster displayed in (A) in the systole (orange) and diastole (blue) as a function of awareness; error bars display the standard error; **p<0.01

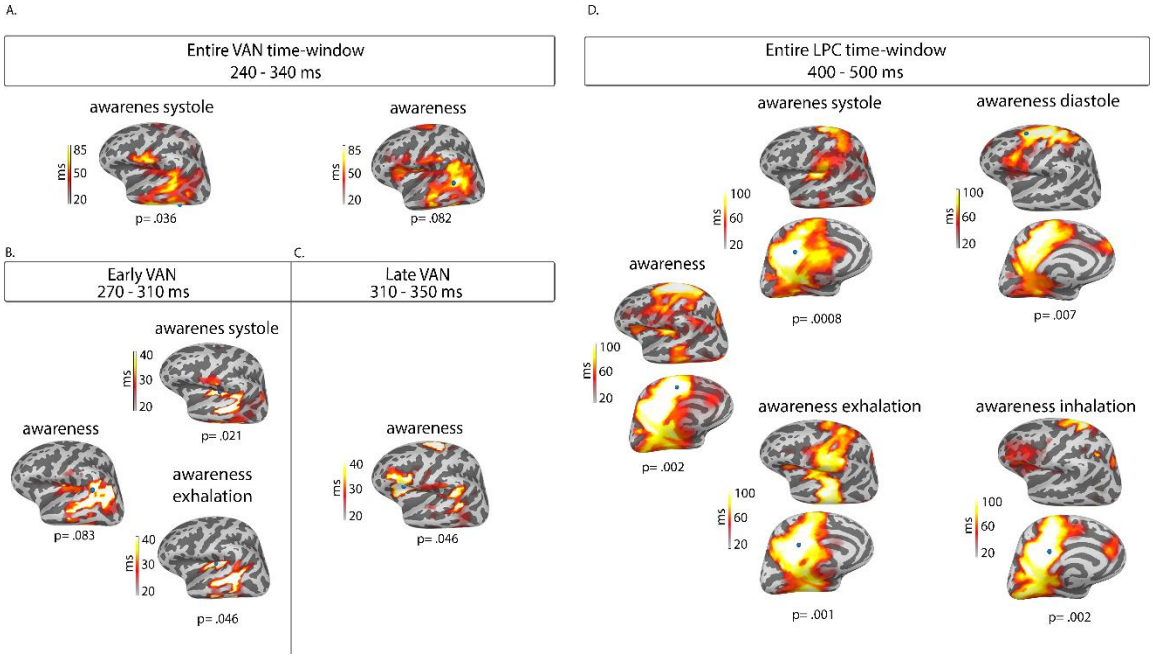

Fig 4. Current density differences underlying the main effect of awareness as a function of the cardiac and respiratory phase for the VAN and P3/LPC components rendered on the FsAverage surface template; color bars indicate the duration (>20 ms) of significant activity in the spatio-temporal clusters between the aware and unaware conditions at the respective significance level. (A) Main effect of awareness in the systole (left) and across all conditions (right) during VAN time-window (240-340 ms). (B) Main effect of awareness during the early VAN time window (rising phase, 270-310 ms) across all conditions (left) and separately for the systole (right top) and exhalation (right bottom). (C) Main effect of awareness in the late VAN time window (310-350 ms) across all conditions. (D) Main effect of awareness during the entire LPC window (400-500 ms) across all conditions (left), for the systole (middle top), diastole (right top), exhalation (middle bottom) and inhalation (right bottom).

SI Results

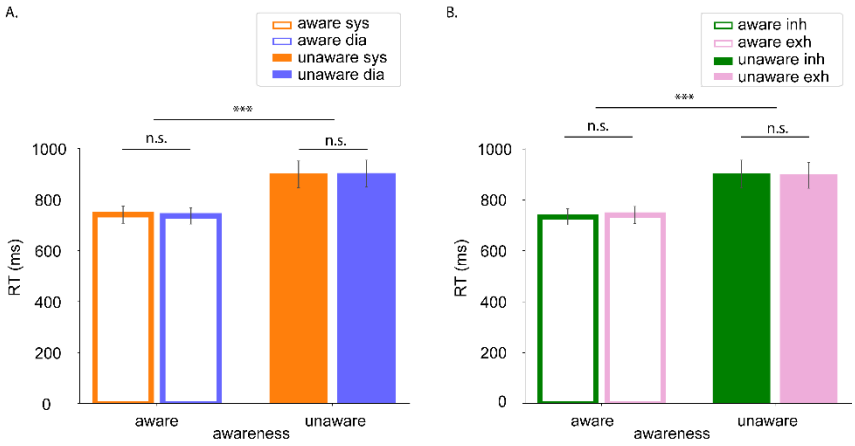

Figure S1. Behavioral results: reaction times (in ms) as a function of awareness and (A) cardiac phase (systole: orange, diastole: blue) and (B) respiratory phase (inhalation: green, exhalation (pink)). The error bars represent the standard error, *** p<.001.

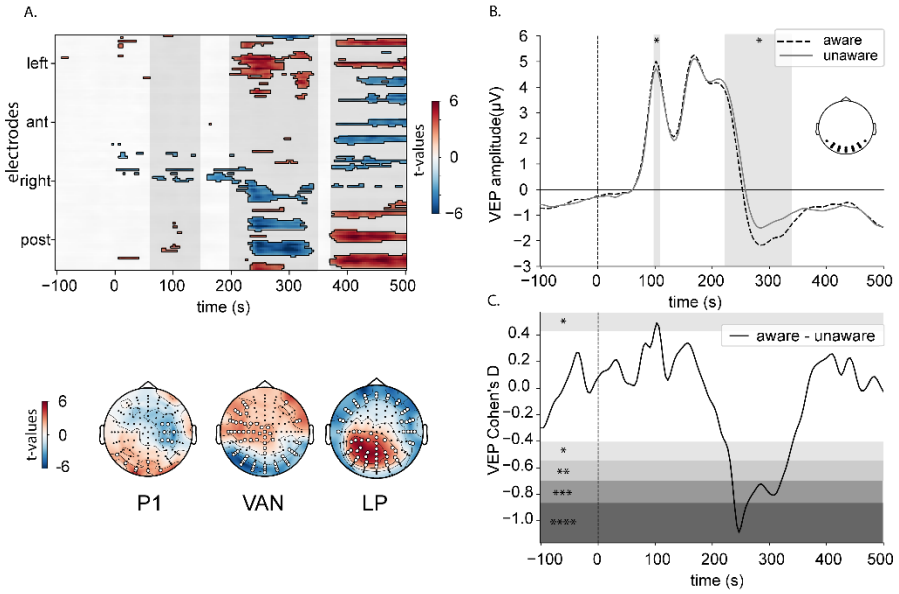

Figure S2. Main effect of awareness on ERP amplitudes. (A) Time-course and location of significant differences for the contrast between aware and unaware identification; top panel: t-values denoting the direction of the main effect (identified by mass univariate ANOVAs, FDR corrected across time and space)); three periods of significant amplitude differences are highlighted in gray: P1 (90 – 120 ms) VAN (250 – 350 ms), P3/LPC (400 – 500 ms), bottom panel: topo-maps illustrating the distribution of the main effects; electrodes showing a significant electrodes main effect of awareness are highlighted by a white circle. (B) Grand average ERP waveforms averaged across the electrodes showing a main effect of awareness in the time-window of the VAN (250 – 350ms) displayed in the inset (C) Time-course of Cohen's d effect sizes for the contrast aware – unaware at the electrodes highlighted in the inset in panel (B); gray shades indicate significance levels (*p<0.05, * p<0.01, ***p<0.001, ****p< 0.0001).

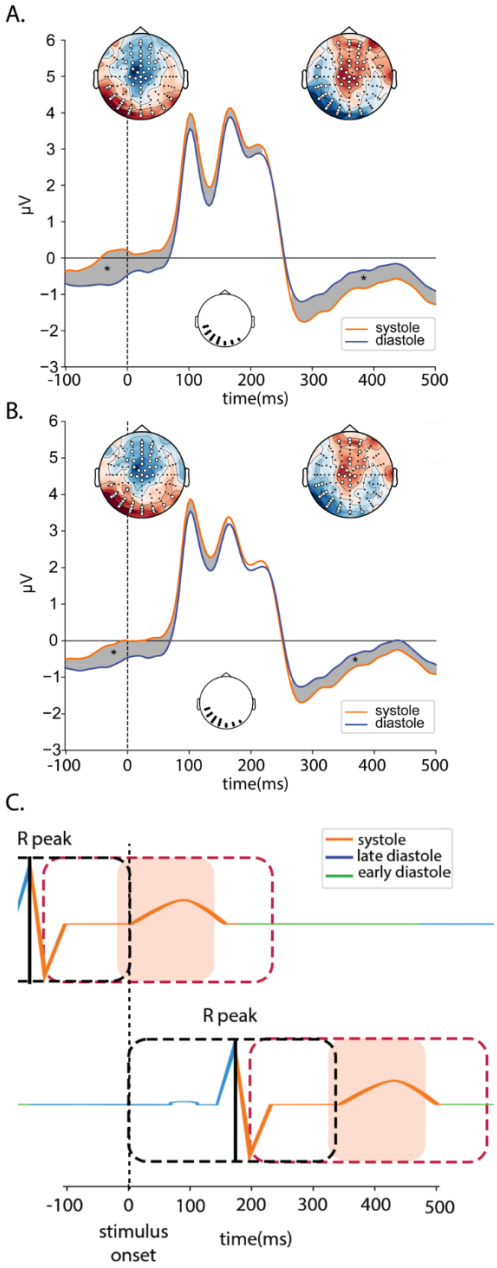

Figure S3. Main effect of cardiac phase on ERPs. (A) Grand Average ERP waveforms averaged across the occipito-temporal electrodes highlighted in the insert in the systole (orange) and diastole (blue) without correction of the cardiac field artifact (CFA). Gray shades indicate time-periods of a significant main effect of cardiac phase identified by mass univariate ANOVAs (FDR corrected), topoplots illustrate the distribution of the main effect, electrodes showing a significant main effect of awareness are highlighted by a white circle. (B) Grand Average ERP waveforms averaged across the occipito-temporal electrodes highlighted in the insert in the systole (orange) and diastole (blue) with correction of the CFA. (C) Illustration of the time-course of the cardiac pulse wave relative to stimulus onset. The dotted black line denotes stimulus onset; the dashed black and red windows denote the time window in which the R peaks and the ensuing pulse waves can occur for stimuli falling into the systole (top panel) and diastole (bottom panel); the solid black line and the orange highlight indicate an exemplar R peak and pulse wave in each condition; note how the significant main effect of cardiac phase in panels (A) and (B) align with the red dashed windows in panel (C).

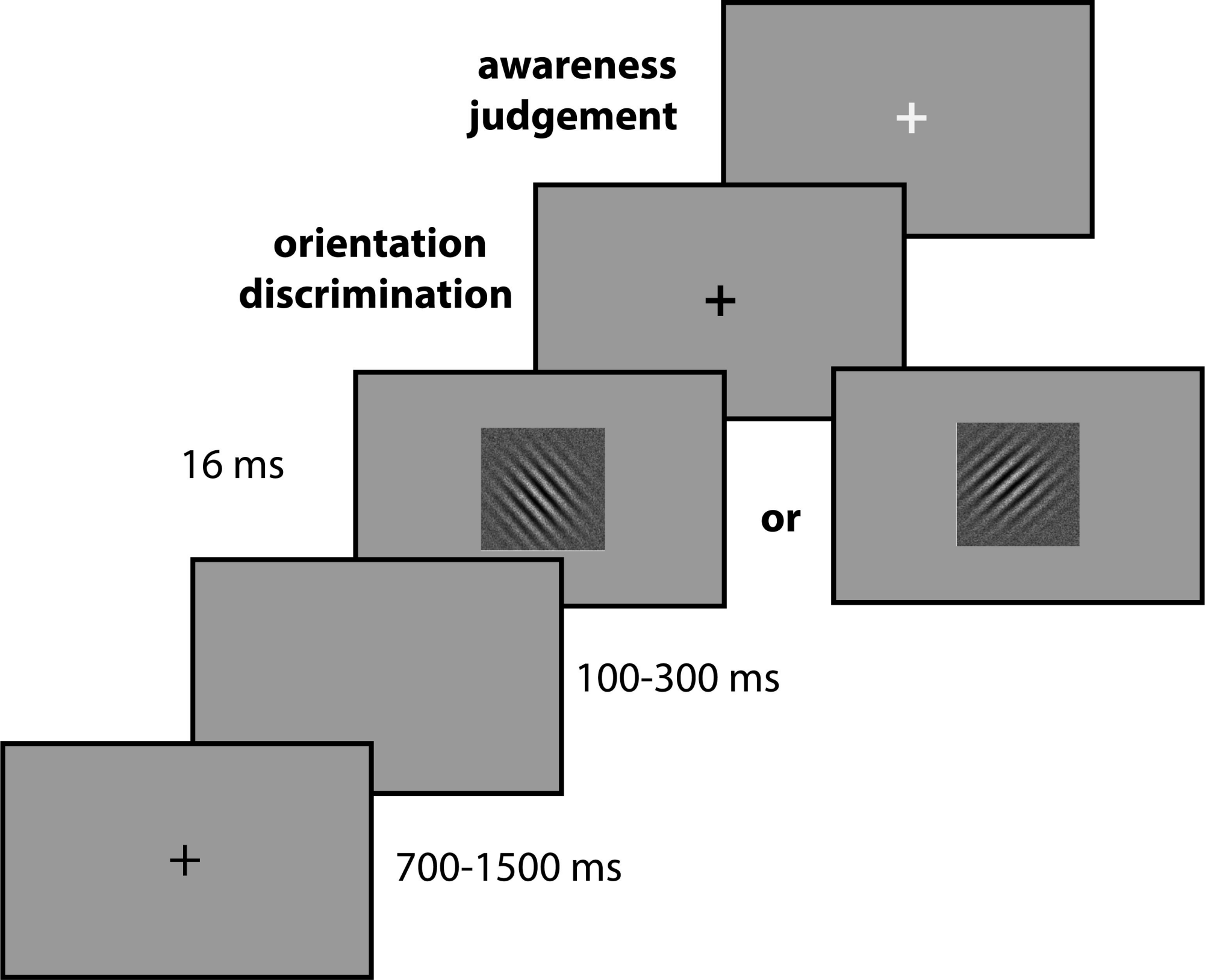
awareness
judgement
orientation
discrimination
16 ms
or
100-300 ms
700-1500 ms

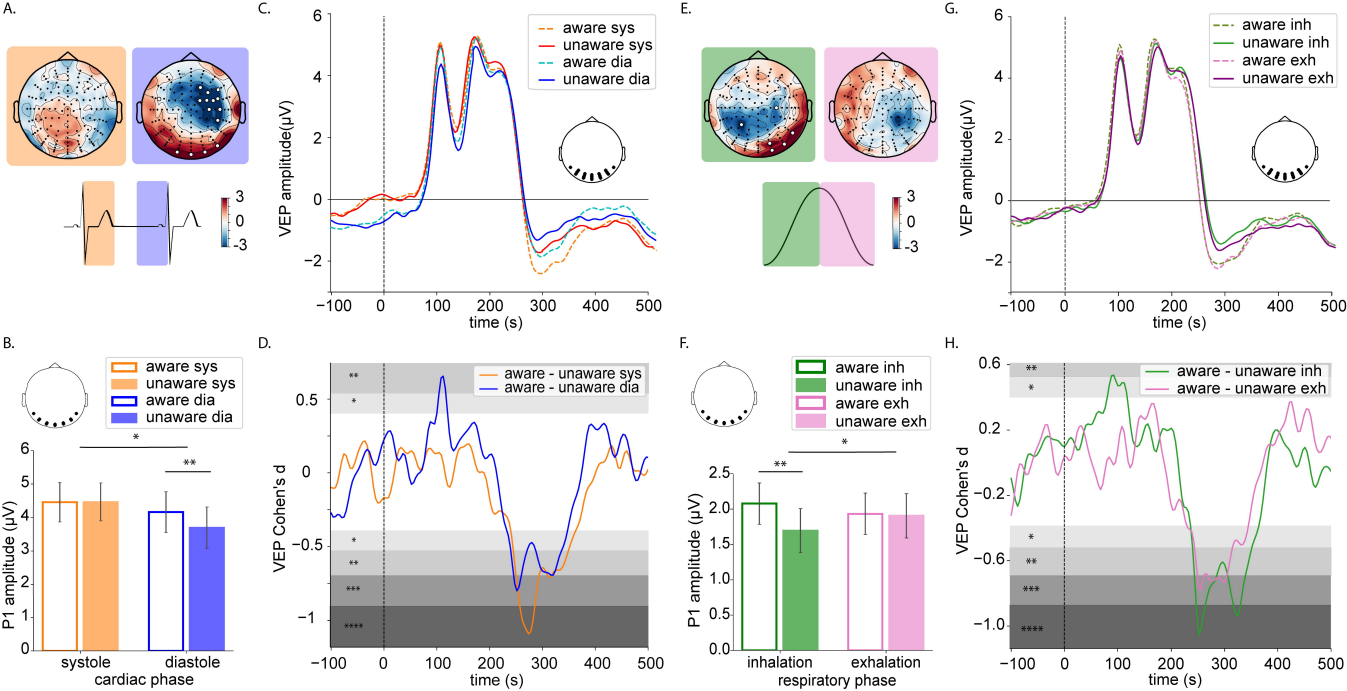
A.
3
0
-3
C.
aware sys
unaware sys
aware dia
unaware dia
VEP amplitude(μV)
time (s)
E.
3
0
-3
G.
aware inh
unaware inh
aware exh
unaware exh
VEP amplitude(μV)
time (s)
B.
aware sys
unaware sys
aware dia
unaware dia
P1 amplitude (μV)
systole
diastole
cardiac phase
D.
aware - unaware sys
aware - unaware dia
VEP Cohen's d
time (s)
F.
aware inh
unaware inh
aware exh
unaware exh
P1 amplitude (μV)
inhalation
exhalation
respiratory phase
H.
aware - unaware inh
aware - unaware exh
VEP Cohen's d
time (s)

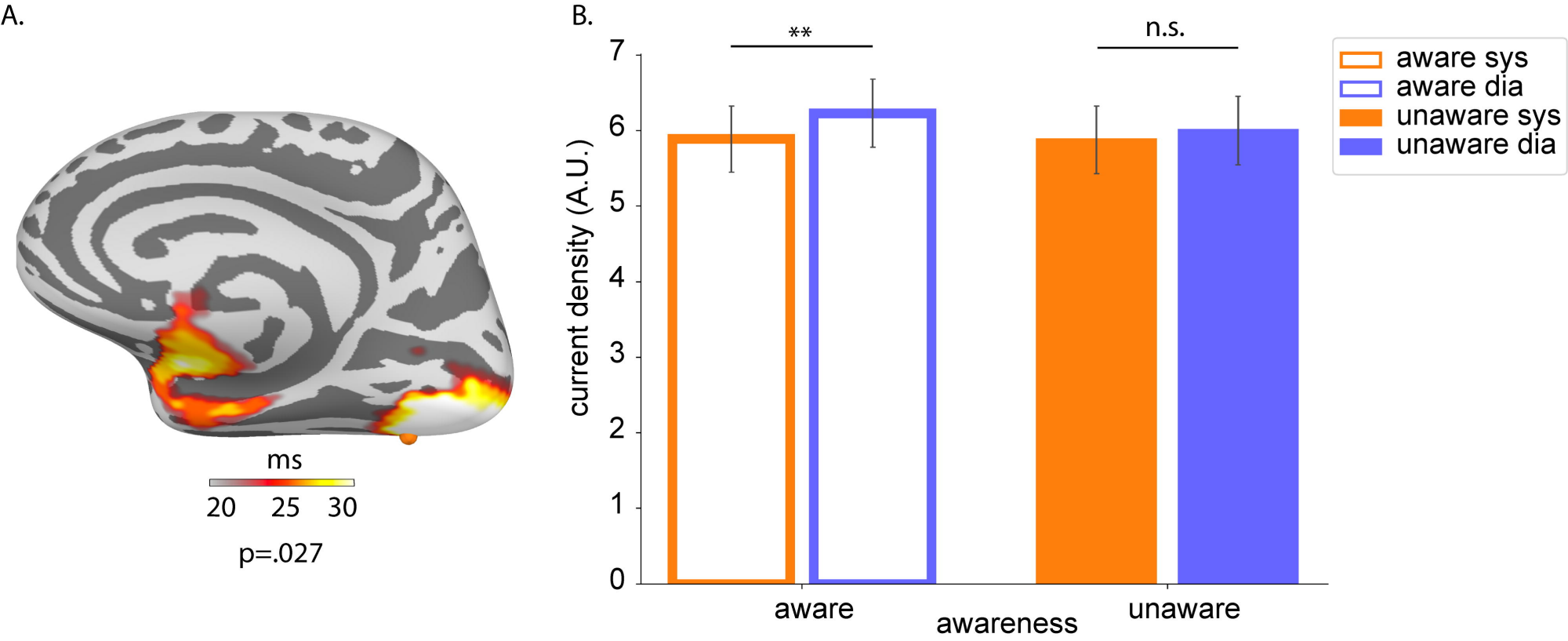
A.
ms
20
25
30
p=.027
B.
**
n.s.
current density (A.U.)
0
1
2
3
4
5
6
7
aware
unaware
awareness
aware sys
aware dia
unaware sys
unaware dia

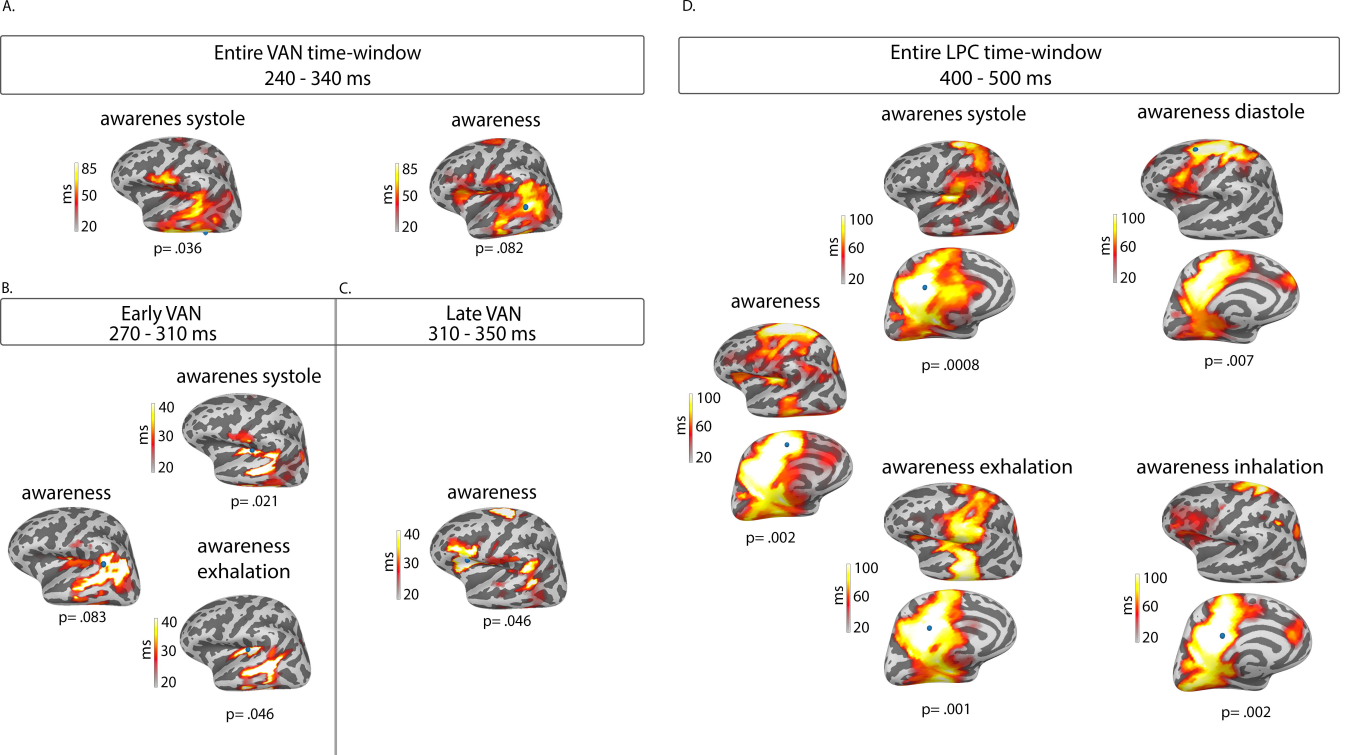
A.
Entire VAN time-window
240 - 340 ms
awarenes systole
ms
85
50
20
p= .036
awareness
ms
85
50
20
p= .082
B.
Early VAN
270 - 310 ms
awarenes systole
ms
40
30
20
p= .021
awareness
p= .083
awareness
exhalation
ms
40
30
20
p= .046
C.
Late VAN
310 - 350 ms
awareness
ms
40
30
20
p= .046
D.
Entire LPC time-window
400 - 500 ms
awarenes systole
ms
100
60
20
p= .0008
awareness diastole
ms
100
60
20
p= .007
awareness
ms
100
60
20
p= .002
awareness exhalation
ms
100
60
20
p= .001
awareness inhalation
ms
100
60
20
p= .002